Scientific Research Publishing

Open Journal of Modelling and Simulation, 2026, 14(3), 73-83
https://www.scirp.org/journal/ojmsi
ISSN Online: 2327-4026
ISSN Print: 2327-4018

# Conservation of Energy in a Closed Universe and the Kinematic Illusion of Dark Energy

**André P. Steynberg**

Dublin, OH, USA
Email: ap.steynberg@gmail.com

**How to cite this paper:** Steynberg, A.P. (2026) Conservation of Energy in a Closed Universe and the Kinematic Illusion of Dark Energy. *Open Journal of Modelling and Simulation*, **14**, 73-83.
https://doi.org/10.4236/ojmsi.2026.143005

**Received:** March 30, 2026
**Accepted:** May 6, 2026
**Published:** May 9, 2026



## Abstract

We explore the thermodynamic lifecycle and macroscopic topology of a closed, temporally bifurcated spacetime manifold by applying the First Law of Thermodynamics and the Principle of Least Action to the primordial photon field. Utilizing a dimensionless equation linking the cosmic scale to the Planck scale, we demonstrate a linear geometric ratio mirroring the Schwarzschild geometry, necessitating a total invariant mass of $2M_u$. To explain this physically, we propose a temporally bifurcated universe originating from a shared 5D torsion axis, which strictly separates a matter hemisphere from an equal antimatter hemisphere, thereby structurally bypassing the need for the Sakharov conditions to resolve Baryon Asymmetry. By evaluating the isotropic radiation pressure of the CMB traversing lines of zero spacetime interval, we offer a mathematical consistency argument—supported by the Isaacson effective stress-energy formulation—that the energy lost by the photon field is conserved as the mechanical work required to drive spherical volume expansion against the 5D Planck Stiffness ( $\kappa_T = c^4/G$ ). Finally, we establish a temporal and spatial boundary ( $z \geq 1$ ) for the application of this pure global expansion. At later historical times, isotropic expansion is superseded by localized gravitational clustering. By analyzing the Milky Way's vantage point near the boundary of the Local Void, we provide quantitative scale checks demonstrating that the apparent "accelerated expansion" of nearby supernovae is a localized kinematic artifact—a bulk flow phenomenon—rendering the hypothesis of Dark Energy unnecessary.

## Keywords

Geometric Monism, Baryon Asymmetry, Closed Universe, Action Principle, Dark Energy, Local Void, Type Ia Supernovae, Bulk Flow

## 1. Introduction: The Dimensionless Geometric Ratio

The macroscopic topology of the universe can be formally constrained by a unified

5D Planck Stiffness ( $\kappa_T = c^4/G$ ) [1]. To complete this physical framework, the microscopic topological constraints must be formally reconciled with the macroscopic boundary conditions of the universe. In earlier work, a dimensionless equation was derived linking the maximum parameters of a closed, finite spacetime manifold to the minimum Planck units [2]:

$$\frac{M_u}{m_P} = \frac{t_m}{\pi t_P} = \frac{l_m}{\pi l_P} \tag{1}$$

where $M_u$ is the mass of the observable universe, $t_m$ is the maximum time dimension, and $l_m$ is the maximum photon distance.

The appearance of $\pi$ in Equation (1) is an artifact of mapping a linear measurement to the spherical geometry of a 3-sphere manifold. When we compare the radial geometry directly, the maximum radius of the finite manifold $R_m$ relates to the maximum time $t_m$ via the circumference ( $R_m = 2ct_m/\pi$ ). By isolating $t_m$ from Equation (1) and substituting it into this geometric relation, the $\pi$ terms cleanly cancel. Because the Planck length $l_P = ct_P$ , we derive the exact ratio between the radius of the macroscopic spacetime manifold and the Planck-scale torsion element:

$$\frac{R_m}{l_P} = 2\left(\frac{M_u}{m_P}\right) \tag{2}$$

The emergence of the factor of 2 is the exact geometric signature of the macroscopic Schwarzschild radius ( $R = 2GM/c^2$ ). As formally proven in **Appendix A**, this is not an invalid application of a local static vacuum metric, but the strict analytical limit of the Friedmann equation evaluated at the global spatial maximum expansion ( $\dot{R} = 0$ ).

## 2. The Antimatter Hemisphere and Temporal Bifurcation

Standard cosmology is plagued by the Baryon Asymmetry problem. Standard baryogenesis models require the Sakharov conditions (baryon number violation, CP violation, and thermal non-equilibrium) to dynamically generate an imbalance from an initially mixed bath of matter and antimatter occupying the same 4D spatial volume.

Geometric Monism offers a topological resolution that is consistent with Equation (2) while offering a topological alternative to these fine-tuned microphysical requirements. We hypothesize that the universe operates as a strictly closed system with a total mass of $2M_u$ , containing exactly equal quantities of matter and antimatter.

### The 5D Emergence Poles and the Shared Torsion Axis ( $r_{\min} = l_P$ )

At the conclusion of the previous spatial contraction cycle, the total energy of the universe is compressed into a primordial matter quark-gluon plasma and an equal antimatter quark-gluon plasma. These states are connected exclusively through a shared 5D torsion axis of radius $r_{\min} = l_P$ . This absolute minimum geometric

boundary physically prevents an infinite-density singularity.

At this temporal origin, the macroscopic matter and antimatter universes do not occupy the same 4D spatial volume; rather, they share the common central axis and immediately traverse in opposite temporal directions ( $+t$ and $-t$ ). Because they are topologically separated at emergence, their inverted chiralities never destructively interfere within the same 4D spacetime, geometrically preventing immediate total annihilation, as illustrated in **Figure 1**. The observed "asymmetry" is merely a local illusion resulting from our confinement entirely within the $+t$ temporal hemisphere.

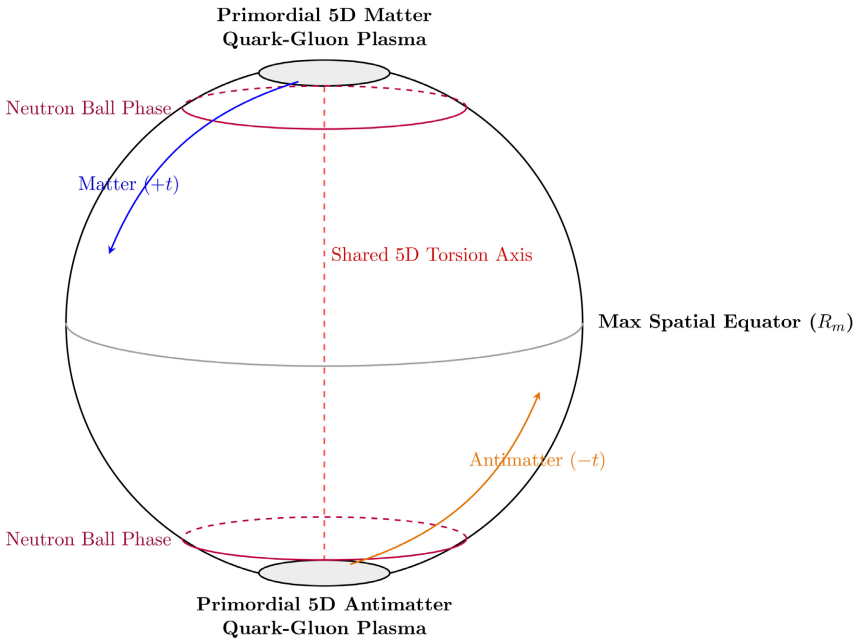


**Figure 1.** Temporal bifurcation on a truncated spacetime manifold (simplified by showing only one of the three identical space dimensions). The matter and antimatter hemispheres traverse opposite temporal longitudes until reaching the maximum spatial equator ( $R_m$ ), which enforces a gravitational turnaround.

## 3. Foundational Thermodynamic Assumptions

Standard cosmology relies on the Friedmann equations, where redshifted photon energy is purportedly lost to "metric expansion" because global energy conservation cannot be formally defined in a non-stationary FLRW spacetime [3]. However, this limitation arises from a geometric asymmetry: standard models treat space as curved and potentially closed, while treating time as an infinite, uncurved coordinate.

The present framework adopts the simplest symmetric assumption: time possesses exactly equal curvature to space. By modeling the universe as a fully closed $S^3$ manifold embedded within a 5D bulk, metric expansion is not a passive coordinate scaling, but a physical stretching of the manifold. Integrating the local covariant conservation law ( $\nabla_\mu T^{\mu\nu} = 0$ ) over this strictly finite volume yields a

globally conserved quantity. We establish the following assumptions:

1) **Total Mass Conservation:** The universe maintains a strictly conserved total invariant mass of $M_{total} = 2M_u$, defined exactly at the primordial temporal pole prior to expansion.

2) **Thermodynamic Isolation:** The 3-sphere is perfectly adiabatic ($dQ = 0$). Energy is exclusively transferred between the internal radiation field and the geometric curvature of the manifold, without exchanging heat with the 5D bulk.

3) **Strict Zero-Interval Propagation:** The spatial traversal of photons ($dx$) is exactly bounded by their temporal traversal ($dt$), guaranteeing isotropic radiation pressure enforces spherical volume expansion.

## 4. Thermodynamic Work and the Adiabatic Expansion of Space

Because the manifold is thermodynamically isolated ($dQ = 0$), the First Law of Thermodynamics dictates that any change in the internal energy ($dU$) of the primordial photons must be offset by the mechanical work done by the system:

$$dU + pdV = 0 \tag{3}$$

For relativistic photons ($p = U/3V$), integrating this relationship yields $U \propto V^{-1/3}$. Because the spatial volume of a 3-sphere is proportional to the cube of its radius ($V \propto R^3$), we find:

$$U \propto \frac{1}{R} \tag{4}$$

The macroscopic wavelength of the primordial photon field must scale linearly with the radius of the universe. The energy lost by the CMB photons is perfectly conserved as the mechanical work required to expand the spatial fabric of the manifold.

### The Energy Equivalence of Planck Stiffness

Treating the geometric expansion of spacetime as mechanical work against a structural stiffness is not a Newtonian analogy, but a rigorous feature of relativistic continuum mechanics explicitly established by the Isaacson equation for gravitational waves [4]. The effective stress-energy tensor of a geometric metric perturbation ($h_{\alpha\beta}$) is defined as:

$$T_{\mu\nu}^{(GW)} = \frac{c^4}{32\pi G}\left\langle \partial_\mu h_{\alpha\beta} \partial_\nu h^{\alpha\beta} \right\rangle \tag{5}$$

This demonstrates that General Relativity natively translates geometric metric evolution into physical thermodynamic energy by multiplying the squared geometric gradient by the absolute Planck Stiffness ($\kappa_T = c^4/G$). In a finite, closed 3-sphere, the macroscopic expansion acts as a global geometric deformation. Therefore, the radiation pressure of the CMB performs tangible mechanical work ($-pdV$) against this exact relativistic stiffness to drive the metric expansion.

## 5. Pseudo-Riemannian Geometry and Null Geodesics

To visualize how the radiation pressure enforces a perfectly isotropic spherical expansion, we must review the invariant spacetime interval ( $ds^2$ ), defined by the metric tensor $g_{\mu\nu}$:

$$ds^2 = g_{\mu\nu} dx^\mu dx^\nu \tag{6}$$

For a massless particle such as a photon, the trajectory is a null geodesic ( $ds^2 = 0$ ). In conformally flat space, this reduces Equation (6) to:

$$c^2 dt^2 - dx^2 = 0 \Rightarrow dx = cdt \tag{7}$$

This invariant zero interval is visualized in **Figure 2**.

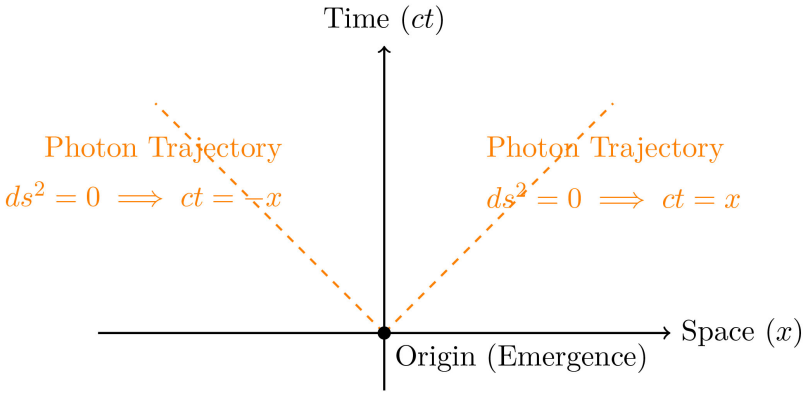


**Figure 2.** A 1 + 1D pseudo-Riemannian spacetime diagram. The invariant zero interval ( $ds^2 = 0$ ) of the photon explicitly geometrically bounds the maximum spatial traversal ( $dx$ ) to the temporal traversal ( $cdt$ ).

In our closed, temporally bifurcated 3-sphere, Equation (7) ensures that spatial expansion is intrinsically bound to temporal traversal. As the initial expansion begins, each fundamental element of matter traces its own distinct temporal path. These individual timelike worldlines are geometrically represented as distinct lines of longitude tracing the surface of the expanding 3-sphere.

While massive particles trace these distinct longitudinal worldlines, the primary photon paths traverse both longitude and latitude at an equal metric rate. This invariant zero interval causes the photon trajectories to act as rigid geometric boundaries, carving the surface of the 3-sphere into expanding operational quadrants, as depicted in **Figure 3**.

## 6. The Ultimate Dimensionless Symmetry and Action Formulation

We can unify this entire lifecycle using the Principle of Least Action ( $\delta S = 0$ ). The total action $S$ for our closed universe system can be expressed as:

$$S = \int \left( \frac{\kappa_T}{16\pi} R + \mathcal{L}_{rad} \right) \sqrt{-g}\, \mathrm{d}^4 x \tag{8}$$

where $R$ is the Ricci scalar curvature and $\mathcal{L}_{rad}$ is the Lagrangian density of the

primordial radiation field. By varying this action with respect to the metric tensor, the geometric curvature of the manifold ( $R$ ) is forced into strict dynamical equilibrium with the stress-energy tensor of the photons.

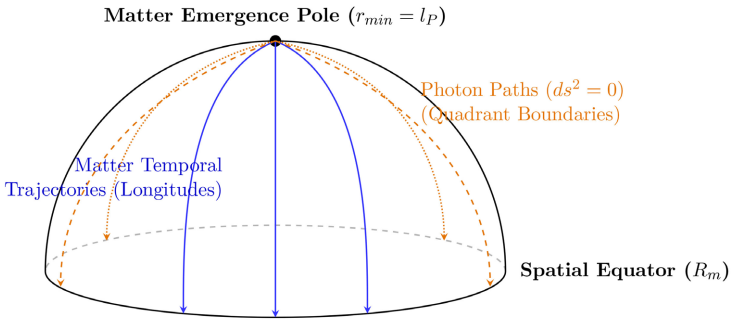


**Figure 3.** Macroscopic mapping of the matter hemisphere. The four distinct primordial photon paths ( $ds^2 = 0$ ) propagate outward, carving the expanding 3-sphere into distinct operational quadrants until the longitudinal traversal halts at the spatial equator ( $R_m$ ).

By defining the total mass of the initial state as $M_{total} = 2M_u$ , we substitute this into our radial ratio (Equation (2)):

$$\frac{R_m}{l_P} = \frac{M_{total}}{m_P} \tag{9}$$

At this spatial equator, the macroscopic radius ( $R_m$ ) is exactly the fundamental torsion radius ( $l_p$ ) scaled linearly by the ratio of the universe's total mass to the Planck mass.

At this critical boundary, the gravitational potential of the $2M_u$ total mass exactly equals the kinetic energy of the expansion, overcoming the diminished radiation pressure. This equator acts as a macroscopic Schwarzschild reflection limit, enforcing a gravitational turnaround and initiating the spatial contraction cycle. Because the matter and antimatter hemispheres are separated temporally rather than spatially, no spatial annihilation boundary exists across the observable universe, natively explaining the lack of gamma-ray annihilation signatures.

## 7. The Breakdown of Isotropic Kinematics

The single-parameter closed universe model provides a geometric fit for cosmic expansion in the early universe, consistent with reported JWST observations of massive galaxies at extreme redshifts ( $z \geq 15$ ) [5]. During the early universe ( $z \gg 1$ ), the global matter distribution was highly uniform, and spatial expansion was purely adiabatic, driven uniformly by the isotropic radiation pressure against the 5D Planck Stiffness.

The model defines redshift as:

$$1 + z = \frac{\sin\left(\frac{13.8}{T} \cdot \frac{\pi}{2}\right)}{\sin\left(\frac{t}{T} \cdot \frac{\pi}{2}\right)}$$

This assumes that the Big Bang (time zero) was 13.8 billion years ago.

The scale factor is:

$$a(t) = \sin\left(\frac{\pi t}{2T}\right)$$

At $t = T$, $a = 1$, and the 3-sphere's radius is:

$$R_m = \frac{2T}{\pi}$$

However, at a critical epoch, localized gravitational attraction began to overpower this uniform thermodynamic expansion, leading to the formation of the "cosmic web" and the evacuation of vast cosmic voids. To preserve the mathematical rigor of cosmic expansion models, data fitting for pure isotropic expansion must be restricted to redshifts $z \geq 1$.

This boundary is supported by large-scale structure formation literature. In N-body simulations (e.g., the Millennium Simulation), the epoch around $z \approx 1$ marks the critical transition where non-linear structure formation begins to radically dominate the universe's matter distribution [6]. For observational data closer to the present time ($z < 1$), non-linear void evacuation and supercluster virialization dominate, and peculiar velocities of bulk flows become a significant, contaminating fraction of the measured recession velocity.

## 8. Re-Evaluating Late-Stage Redshift Data

### 8.1. Methodology and Target Observables

The foundational evidence for an accelerating universe—and consequently, Dark Energy—relies primarily on the luminosity-distance residuals of Type Ia Supernovae (SNe Ia) located at relatively low redshifts ($z < 1$). Standard models fit these observables to a Hubble diagram, assuming deviations from a linear Hubble law result from a changing global expansion rate ($\Lambda$). To extract this global metric, peculiar-velocity corrections are applied to subtract local kinematic motion.

The methodology of this framework involves testing whether the peculiar-velocity corrections applied to $z < 1$ SNe Ia datasets are fundamentally contaminated by the Milky Way's specific kinematic environment, mapped by recent large-scale cosmography surveys.

### 8.2. Quantitative Scale Check of Kinematic Contamination

At a benchmark redshift of $z \approx 0.05$, the deviation from a linear Hubble flow required to fit the $\Lambda$CDM model corresponds to a distance modulus residual of approximately ~0.05 to 0.1 magnitudes [7] [8]. Kinematically, this translates to an apparent excess recession velocity of roughly $\Delta v_{\Lambda} \approx 200$ - 400 km/s.

The Milky Way does not reside in a region of uniform density; we are located on the edge of the vast Local Void, deeply embedded within the branching structure of the massive Laniakea Supercluster [9] [10]. The measured peculiar velocity of the Local Group—driven by gravitational repulsion from the void and attraction

toward Shapley—is empirically established at approximately $v_{pec} \approx 630$ km/s [11].

This numerical scale check demonstrates that the amplitude of our localized macroscopic bulk flow (>600 km/s) is greater than the velocity residual attributed to Dark Energy at these redshifts. If cosmological fits systematically underestimate this coherent bulk flow, the uncorrected kinematic drift will organically reproduce the observational signature of an accelerating spatial expansion of the universe.

## 9. Kinematic Monopoles, Dipoles, and Apparent Isotropy

A common defense of Dark Energy is the apparent isotropy of the acceleration signal. If the Milky Way is subject to a directional bulk flow toward Laniakea, one might expect a purely dipole acceleration signature. However, this expectation overlooks the dual kinematic nature of our environment.

The Milky Way is embedded on the boundary of the Local Void. A cosmic void evacuates matter radially outward, generating a localized kinematic "bubble" characterized by a monopole expansion. Consequently, nearby galaxies in nearly all directions are pushed away from the void's center, receding faster than the baseline global Hubble flow.

When standard models spherically average SNe Ia calibrators, the directional dipole is smeared, and the localized monopole is mathematically misinterpreted as a uniform global acceleration ($\Lambda$). Furthermore, when SNe Ia data is analyzed without assuming strict isotropy, the acceleration signal is significantly anisotropic. Colin *et al.* (2019) demonstrated a pronounced dipole in the deceleration parameter ( $q_0$ ), with the axis of maximum apparent acceleration aligning directly with our local bulk flow [12]. This strongly supports the hypothesis that the Dark Energy signal is deeply contaminated by localized kinematics.

## 10. Consistency with CMB and BAO Probes

Standard cosmology cross-validates Dark Energy using the Cosmic Microwave Background (CMB) and Baryon Acoustic Oscillations (BAO). In $\Lambda$CDM, Dark Energy ( $\Omega_\Lambda \approx 0.68$ ) is mathematically required to bring the total energy density to exactly $\Omega = 1$, yielding a flat geometry that fits the angular position of the CMB's first acoustic peak.

However, in a natively closed 3-sphere ( $k = +1$ ), spatial curvature intrinsically shifts the angular scale, satisfying the position of the acoustic peak without requiring an arbitrary $\Lambda$ term to pad the energy density. Recent analyses of Planck data have independently highlighted that a closed universe provides a highly consistent fit to the CMB power spectrum [13].

Furthermore, as mathematically detailed in **Appendix B**, when local bulk-flow kinematics are subtracted from low-redshift BAO anchoring data, and the transverse distance is modeled via the native $S^3$ trigonometric projection, apparent BAO acceleration anomalies natively resolve into the static geometric curvature of the closed manifold.

## 11. The Minor Thermodynamic Contribution of Galactic Photons

While macroscopic expansion is overwhelmingly driven by the isotropic radiation pressure of the CMB, the cumulative emission of stellar photons (Extragalactic Background Light) introduces a supplementary thermodynamic variable. Because these galactic photons increase the total internal energy ( $U$ ) of the closed manifold, they exert an additional fractional radiation pressure against the 5D Planck Stiffness.

However, the absolute maximum number of photons that galaxies can inject is dwarfed by the primordial CMB photon-to-baryon ratio ( $\eta \approx 10^9 : 1$ ). Therefore, while the EBL provides a minor supplementary thermodynamic pressure—contributing to a slight enhancement in the expansion of space relative to the pure CMB baseline—it is historically negligible compared to the primary driver.

## 12. Conclusions

By synthesizing finite cosmological boundaries with the thermodynamic rules of a perfectly adiabatic system, we argue that the universe possesses strict geometric and temporal symmetry. The dimensionless ratio predicts a temporally bifurcated $2M_u$ mass geometry, elegantly resolving the Baryon Asymmetry problem without unobserved microphysics.

The macroscopic lifecycle guarantees global energy conservation, while establishing a firm temporal threshold ( $z = 1$ ) for pure isotropic thermodynamics. The late-time enhanced separation of galaxies observed from Earth is the deterministic kinematic result of non-linear macroscopic clustering. By recognizing our specific vantage point on the edge of the Local Void, we provide a strongly competitive theoretical alternative to the Dark Energy hypothesis, preserving a conserved-energy interpretation to cosmological mechanics.

## Conflicts of Interest

The author declares no conflicts of interest regarding the publication of this paper.

## References

[1] Steynberg, A.P. (2026) Geometric Monism: A 5-Dimensional Torsion-Based Calculation of Rest Mass for the Standard Model Spectrum. Zenodo. https://doi.org/10.5281/zenodo.18940793

[2] Steynberg, A.P. (2022) A Dimensionless Equation Linking the Maximum and Minimum Values for Mass (or Energy) and Time (or Length). *Global Journal of Science Frontier Research*, **22**, 1-3.

[3] Misner, C.W., Thorne, K.S. and Wheeler, J.A. (1973) Gravitation. W. H. Freeman and Company.

[4] Isaacson, R.A. (1968) Gravitational Radiation in the Limit of High Frequency. II. Nonlinear Terms and the Effective Stress Tensor. *Physical Review*, **166**, 1272-1280. https://doi.org/10.1103/PhysRev.166.1272

[5] Steynberg, A.P. (2025) Single Parameter Model for Cosmic Scale Photon Redshift in

a Closed Universe Applied to Data from JWST. *Open Journal of Modelling and Simulation*, **13**, 204-210. https://doi.org/10.4236/ojmsi.2025.134012

[6] Springel, V., White, S.D.M., Jenkins, A., Frenk, C.S., Yoshida, N., Gao, L., *et al.* (2005) Simulations of the Formation, Evolution and Clustering of Galaxies and Quasars. *Nature*, **435**, 629-636. https://doi.org/10.1038/nature03597

[7] Riess, A.G., Filippenko, A.V., Challis, P., Clocchiatti, A., Diercks, A., Garnavich, P.M., *et al.* (1998) Observational Evidence from Supernovae for an Accelerating Universe and a Cosmological Constant. *The Astronomical Journal*, **116**, 1009-1038. https://doi.org/10.1086/300499

[8] Perlmutter, S., Aldering, G., Goldhaber, G., Knop, R.A., Nugent, P., Castro, P.G., *et al.* (1999) Measurements of $\omega$ and $\lambda$ from 42 High-Redshift Supernovae. *The Astrophysical Journal*, **517**, 565-586. https://doi.org/10.1086/307221

[9] Tully, R.B., Courtois, H., Hoffman, Y. and Pomarède, D. (2014) The Laniakea Supercluster of Galaxies. *Nature*, **513**, 71-73. https://doi.org/10.1038/nature13674

[10] Keenan, R.C., Barger, A.J. and Cowie, L.L. (2013) Evidence for a ~300 Mpc Scale Under-Density in the Local Galaxy Distribution. *The Astrophysical Journal*, **775**, Article 62. https://doi.org/10.1088/0004-637X/775/1/62

[11] Hoffman, Y., Pomarède, D., Tully, R.B. and Courtois, H.M. (2017) The Dipole Repeller. *Nature Astronomy*, 1, Article No. 0036. https://doi.org/10.1038/s41550-016-0036

[12] Colin, J., Mohayaee, R., Rameez, M. and Sarkar, S. (2019) Evidence for Anisotropy of Cosmic Acceleration. *Astronomy & Astrophysics*, **631**, Article No. L13. https://doi.org/10.1051/0004-6361/201936373

[13] Di Valentino, E., Melchiorri, A. and Silk, J. (2019) Planck Evidence for a Closed Universe and a Possible Crisis for Cosmology. *Nature Astronomy*, **4**, 196-203. https://doi.org/10.1038/s41550-019-0906-9

# Appendix

## A. Friedmann Boundary Condition at Maximum Expansion

To demonstrate that the factor of 2 in our dimensionless framework is an intrinsic property of a closed universe, we analyze the standard Friedmann equation for a $k=+1$ geometry:

$$\left(\frac{\dot{R}}{R}\right)^2 = \frac{8\pi G\rho}{3} - \frac{c^2}{R^2} \tag{10}$$

Substituting the volumetric mass density ( $\rho = 3M/4\pi R^3$ ):

$$\left(\frac{\dot{R}}{R}\right)^2 = \frac{2GM}{R^3} - \frac{c^2}{R^2} \Rightarrow \dot{R}^2 = \frac{2GM}{R} - c^2 \tag{11}$$

At the spatial "equator" (global maximum expansion limit), macroscopic expansion must momentarily halt ( $\dot{R}=0$ ). This evaluates the strict boundary condition:

$$0 = \frac{2GM}{R_{\max}} - c^2 \Rightarrow R_{\max} = \frac{2GM}{c^2} \tag{12}$$

This confirms that a closed universe natively recovers the exact mathematical signature of the Schwarzschild radius at its maximum expansion limit.

## B. Kinematic Calibration and the Geometric Resolution of BAO Anomalies

The observed redshift ( $z_{obs}$ ) of a low-redshift BAO calibrator galaxy is a composite of its cosmological metric redshift ( $z_c$ ) and its peculiar kinematic velocity ( $v_{pec}$ ):

$$z_{obs} \approx z_c + \frac{v_{pec}}{c} \tag{13}$$

As established in Section 8.2, an uncorrected bulk flow of $v_{pec} \approx 630$ km/s introduces a systemic kinematic error of $\Delta z_{kin} \approx 0.002$ . Because the local Hubble constant is calibrated as $H_0 \approx cz_{obs}/D$ , artificially inflating $z_{obs}$ systematically overestimates the global expansion rate ( $H_0$ ).

When standard ΛCDM applies this overestimated $H_0$ to high-redshift BAO data, the theoretical distance falls short. In the single-parameter closed universe, the transverse comoving distance $D_M(z)$ must be geometrically projected across the curvature of the 3-sphere radius ( $R_0$ ):

$$D_M(z) = R_0 \sin\left(\frac{\chi(z)}{R_0}\right) \approx \chi(z) - \frac{\chi(z)^3}{6R_0^2} \tag{14}$$

When the baseline expansion rate ( $H_0$ ) is correctly reduced by subtracting the local macroscopic bulk flow, and the transverse distance is modeled via the native $S^3$ trigonometric projection ( $\sin(\chi/R_0)$ ), the apparent BAO acceleration anomaly is absorbed entirely by the static spatial curvature.